



# Soft magnetic (Fe, M)–Y–B (M = Co or Ni) bulk metallic glasses

C.Y. Lin, T.S. Chin\*

*Department of Materials Science and Engineering, National Tsing-Hua University, No. 101, Guang-Fu Road,  
Section 2, Hsinchu 30013, Taiwan, Republic of China*

Received 6 July 2006; received in revised form 30 July 2006; accepted 31 July 2006  
Available online 12 September 2006

## Abstract

Thermal and magnetic properties of  $\text{Fe}_{69-74}\text{Y}_{4-9}\text{B}_{22}$ , and  $(\text{Fe}, \text{M})_{12}\text{Y}_6\text{B}_{22}$  (M = Co or Ni) bulk metallic glasses (BMG) were investigated. The alloys keep the ability to cast BMGs as Co or Ni replacement is up to 36 or 10 at.%. Saturation magnetization decreases from 1.47 T ( $\text{Fe}_{72}\text{Y}_6\text{B}_{22}$ ) to 1.11 T (36 at.% Fe replaced by Co) and to 1.24 T (10 at.% Fe replaced by Ni). The coercivity is 10–40 A/m, the Curie temperature is higher than 535 K, and electrical resistivity is greater than  $200 \mu\Omega \text{ cm}$  for all the studied BMGs. With such promising properties, these alloys are potential for industrial applications.

© 2006 Published by Elsevier B.V.

PACS: 75.50.kj

Keywords: Amorphous materials; Magnetic properties; Bulk metallic glasses; Thermal analysis; Fe–Y–B

## 1. Introduction

Iron-based amorphous magnetic alloys have attracted much attention due to their good soft magnetic properties for industrial applications in transformers and cores. Recently, many bulk metallic glasses (BMG) were developed in multi-component Mg-, Ln- (Ln = lanthanide), Zr- and Pd- and Ti-based alloy systems [1–6]. These BMGs always show wide super-cooled liquid region, that quantifies the degree of resistance against crystallization, leading to a high glass-forming ability (GFA) capable of casting into amorphous rods, a few to a few tens mm in diameter. They exhibit many promising mechanical and/or functional properties.

It has long been desirable to explore iron-based alloys with better GFA to cast bulk Fe-based magnetic BMGs and extend their industrial applicability. Inoue disclosed three empirical rules that govern the GFA of an alloy system: (1) multi-component alloys consist of more than three elements; (2) large difference in atomic size differences, better larger than 12%; (3) large negative heats of mixing [7]. According to these rules, new Fe-based bulk amorphous alloys have been successfully devel-

oped. These alloys are mainly of the three groups of elements: Fe–(Al, Ga)–(P, Si, B, C) [8], Fe–(Co, Ni)–M–B (M = Zr, Hf, Nb, Ta, Mo, W) [9] and Fe–Ni–P–B [10]. However, all these alloys consist of complex composition with at least four constituent elements. Since the successful development in our Laboratory of ternary iron-based bulk metallic glasses, Fe–X–B (X is one of Sc, Y, Dy, Ho and Er) [11,12], Fe–Y–B BMG shows much higher potential in industrial applications than other four systems. It is natural and interesting to examine the effects of replacing part of Fe by other magnetic elements, Co and Ni, on glass forming ability, thermal, magnetic and electrical properties of the Fe–Y–B ternary BMGs. In this paper, effects of the modifications thereof on various properties of the ternary BMG are reported.

## 2. Experimental

Ingots of studied alloys with nominal compositions  $\text{Fe}_{78-x}\text{Y}_x\text{B}_{22}$ ,  $\text{Fe}_{72-y}\text{Co}_y\text{Y}_6\text{B}_{22}$  ( $y = 0, 10, 20, 30, 36, 50$ ) and  $\text{Fe}_{72-z}\text{Ni}_z\text{Y}_6\text{B}_{22}$  ( $z = 5, 10, 15, 20$ ) were prepared by arc melting the mixtures of pure Fe, Co, Y metals and B beads under 0.01 MPa. Ribbons with a cross-section of about  $0.03 \text{ mm} \times 10 \text{ mm}$  were prepared by a single-roller melt-spinning method. Bulk alloys in rod form with different diameters were prepared by conventional injection-casting into a copper mold. The structure was examined by X-ray diffraction (Shimadzu XRD-6000). Thermal properties were studied by differential thermal analysis (DTA, Perkin-Elmer Diamond TG/DTA) at a heating rate 20 K/min. The Curie temperature,  $T_c$ , was measured with a magnetic-thermal-gravimetric analyzer (M-TGA, Perkin-Elmer Pyris 6) at a heating rate 5 K/min. Magnetic properties

\* Corresponding author.

E-mail addresses: [d917517@oz.nthu.edu.tw](mailto:d917517@oz.nthu.edu.tw) (C.Y. Lin),  
[tschin@mx.nthu.edu.tw](mailto:tschin@mx.nthu.edu.tw) (T.S. Chin).

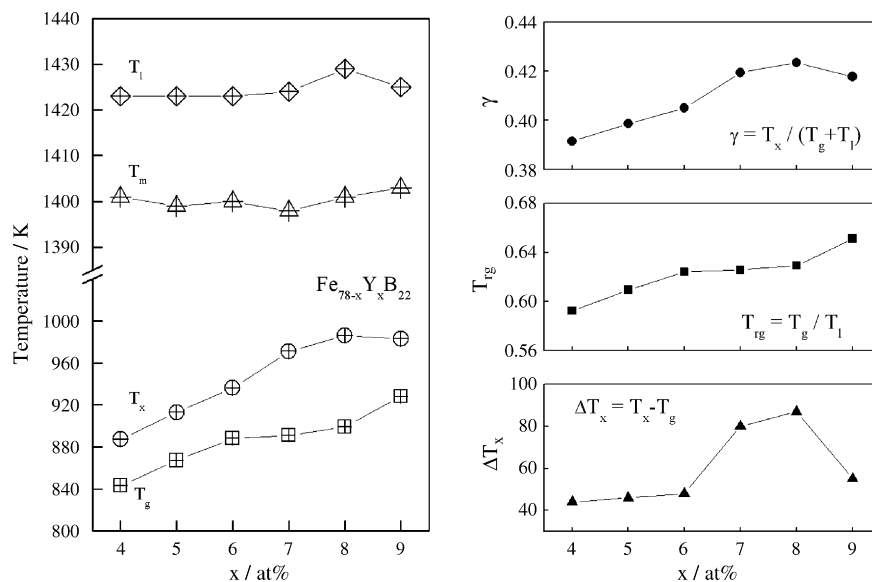


Fig. 1. Thermal properties and the glass forming ability, expressed in different criteria, of  $\text{Fe}_{78-x}\text{Y}_x\text{B}_{22}$  ( $x = 4-9$ ) amorphous ribbons.

were measured with a vibrating sample magnetometer (VSM, Digital Measurement Systems, Model 4HF). The electrical resistivity was measured by a typical four-point probe method.

### 3. Results and discussion

It has been evaluated that the  $\text{Fe}_{78-x}\text{Y}_x\text{B}_{22}$  alloy system exhibit good glass forming ability (GFA) to form bulk glassy rods, at least 1 mm in diameter, in the composition range 4–9 at.% Y content [12]. Fig. 1 shows thermal properties and important factors describing GFA of the  $\text{Fe}_{78-x}\text{Y}_x\text{B}_{22}$  alloy system. Both the glass transition temperature ( $T_g$ ) and crystallization temperature ( $T_x$ ) gradually increases with Y content from 843 to 928 K, and 887 to 986 K, respectively. However, it is unexpected that both the melting point,  $T_m \sim 1400$  K, and liquidus temperature,  $T_l \sim 1425$  K, keep almost unchanged with considerable change in Y content. The super-cooled liquid region ( $\Delta T_x$ ), which is defined as the interval between the  $T_g$  and  $T_x$  ( $\Delta T_x = T_x - T_g$ ), gradually increases with Y content and reaches the maximum value over 80 K as  $x = 7$  and 8 and then decreases. The reduced glass transition temperature,  $T_{rg} (=T_g/T_l)$  and  $\gamma$  factor ( $=T_x/(T_g + T_l)$ ) increase with Y content. However, experimental trials showed that  $\text{Fe}_{72}\text{Y}_6\text{B}_{22}$  ( $x = 6$ ) has the best GFA which is able to form a bulk glassy rod at least 2 mm in diameter by copper mold casting method among the studied ternary Fe–Y–B alloys. Surprisingly, the  $\text{Fe}_{72}\text{Y}_6\text{B}_{22}$  alloy exhibits neither the largest super-cooled liquid region nor the largest reduced glass transition temperature, and not the largest  $\gamma$  value of the  $\text{Fe}_{78-x}\text{Y}_x\text{B}_{22}$  alloy series. These similar phenomena were also found in the Cu–Zr binary BMG system [13]. The reasons for good GFA of Fe–Y–B ternary alloy system have been investigated elsewhere [14]. It is well known that good glass former can be found in deep eutectic systems. These good glass formers locate in the ternary eutectic region of Fe,  $\text{Fe}_2\text{B}$  and  $\text{Fe}_4\text{B}_4\text{Y}$  in the Fe–Y–B system. The pinpointing strategy developed recently [15–19] depicted that the good glass

forming region is surrounded by amorphous composites. And more importantly, there is a switch in phases which involved in the competition of glass formation in Fe–Y–B ternary system. They are the equilibrium phases of Fe,  $\text{Fe}_2\text{B}$  and  $\text{Fe}_4\text{B}_4\text{Y}$ . The glass-forming behavior of Fe–Y–B system is consistent with the case in Zr–Cu–Al ternary BMG system where the best glass forming alloys were found at Al content below 6–8 at.% [18]. All of them are limited by their corresponding ternary triangles. On the other hand, the effects of adding large atoms into Fe–B binary system were also investigated by using the *ab initio* calculation simulation [20]. In the research for Fe-based bulk glass forming alloys, the GFA could be enhanced by destabilizing the Fe–B and Fe–C-based crystalline structures that are based on the structural prototype  $\text{C}_6\text{Cr}_{23}$  which often preempt the amorphous phase. From the first-principle total energy calculation of enthalpy of formation, it was also identified that among the 4d transition metals yttrium is the only element effectively destabilized the  $\text{C}_6\text{Cr}_{23}$ -type structure leading to an improvement in GFA [20]. It was also pointed out that too large an yttrium concentration (9 at.% or more) leads to the formation of other competing crystalline phases such as  $\text{C}_3\text{Fe}_{17}\text{Y}_2$  and leads to a decrement in GFA. These theoretical elucidations are coincidentally consistent with our experimental results. It is also noticed that the value of thermal criteria of ternary Fe–Y–B BMGs are rather high comparing to other kind of Fe-based BMGs with similar GFA (cast diameters) [8–10]. However, the results are fully consist with the results done by other group where the  $\Delta T_x$  is 72 K for the  $\text{Fe}_{70.2}\text{B}_{24}\text{Y}_{5.8}$  alloy and the  $T_{rg} (=T_g/T_l)$  was 0.57 for  $\text{Fe}_{75.7}\text{B}_{20}\text{Y}_{4.3}$  [19]. The reason of smaller cast BMG diameter may come from the simple composition of the alloys. The theoretical analyses mentioned above also have pointed out that too much Y content (9 at.%) leads to the formation of  $\text{C}_3\text{Fe}_{17}\text{Y}_2$  type competing crystalline phase so that thought the alloys  $\text{Fe}_{78-x}\text{Y}_x\text{B}_{22}$ ,  $x = 7, 8$  exhibit the largest  $\Delta T_x$ , they in fact have lower cast diameters than that of  $x = 6$ .

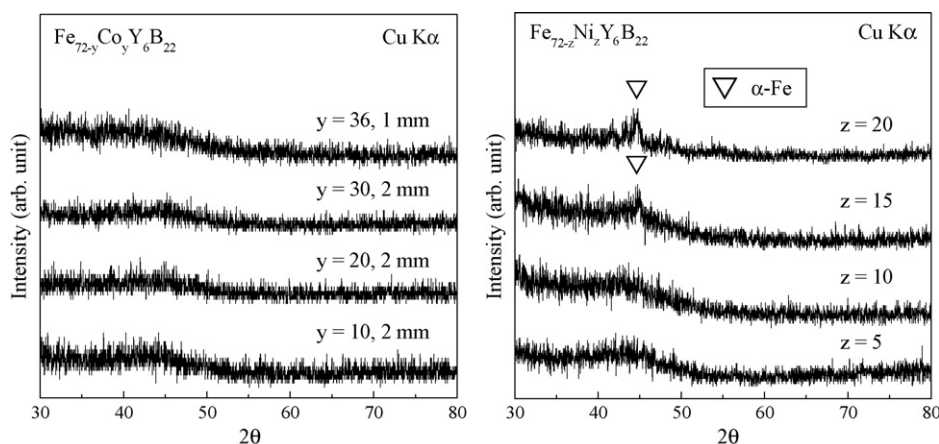


Fig. 2. X-ray diffraction patterns taken on cross-sections of as-cast rods, 1–2 mm in diameter, of  $\text{Fe}_{72-y}\text{Co}_y\text{Y}_6\text{B}_{22}$  alloys ( $y=0\text{--}36$ ); and as-cast 1 mm rods of  $\text{Fe}_{72-z}\text{Ni}_z\text{Y}_6\text{B}_{22}$  alloys ( $z=0\text{--}20$ ).

Fig. 2 shows X-ray diffraction patterns taken on cross-sectional surface of as-cast rods of  $\text{Fe}_{72-y}\text{Co}_y\text{Y}_6\text{B}_{22}$  ( $y=10, 20, 30, 36$ ) and  $\text{Fe}_{72-z}\text{Ni}_z\text{Y}_6\text{B}_{22}$  ( $z=5, 10, 15, 20$ ) alloys. The results show that no obvious diffraction peak was detected by XRD for all Co-modified alloys. This depicts that the Fe–Y–B alloys exhibit a great tolerance in GFA for Fe substitution by Co. The original  $\text{Fe}_{72}\text{Y}_6\text{B}_{22}$  BMG has a GFA capable of casting into amorphous rods at least 2 mm in diameter, being the best among the Fe–Y–B ternary alloys. The alloy retains good GFA to form bulk glassy rods at least 2 mm in diameter as Co content is up to 30 at.%, and at least 1 mm as Co content is further increased to 36 at.%. This means that Co is not harmful to the excellent GFA of the ternary Fe–Y–B BMGs at all. In as-cast rods of 2.5 mm diameter, as Co = 10, 20, 30 at.%, we observed a cored structure with outer glassy regime enclosing an inner crystalline phase. On the other hand, as Fe was substituted by Ni, the GFA was obviously lowered. The largest attainable BMG rods are with

diameter not larger than 1 mm as Ni substitution is 10 at.%. As Ni replacement is higher than 10 at.%,  $\text{Fe}_{72-z}\text{Ni}_z\text{Y}_6\text{B}_{22}$  alloys lose the BMG capability and crystalline  $\alpha\text{-Fe}$  phase appears after casting. During the study, we also observed that the as-cast rods with higher Ni content ( $\text{Ni} > 20$  at.%) become quite brittle. Moreover, it was found that both  $\text{Co}_{72}\text{Y}_6\text{B}_{22}$  and  $\text{Ni}_{72}\text{Y}_6\text{B}_{22}$  ternary alloys can be easily prepared as amorphous ribbons by melt-spinning technique although they are not able to form BMGs by copper mold casting method. It thus requires further investigation to explore simple ternary BMGs of the Co-based and Ni-based alloys.

Fig. 3 shows DTA curves of  $\text{Fe}_{72-y}\text{Co}_y\text{Y}_6\text{B}_{22}$  ( $y=0\text{--}50$ ) and  $\text{Fe}_{72-z}\text{Ni}_z\text{Y}_6\text{B}_{22}$  ( $z=0\text{--}20$ ) amorphous ribbons. Both the crystallization temperature,  $T_x$ , and glass transition temperature,  $T_g$ , decrease with Co or Ni substitution. The crystallization mode changes from multi-stage to single-stage as Co or Ni addition increases. The onset of crystallization temperature,  $T_x$ , decreases

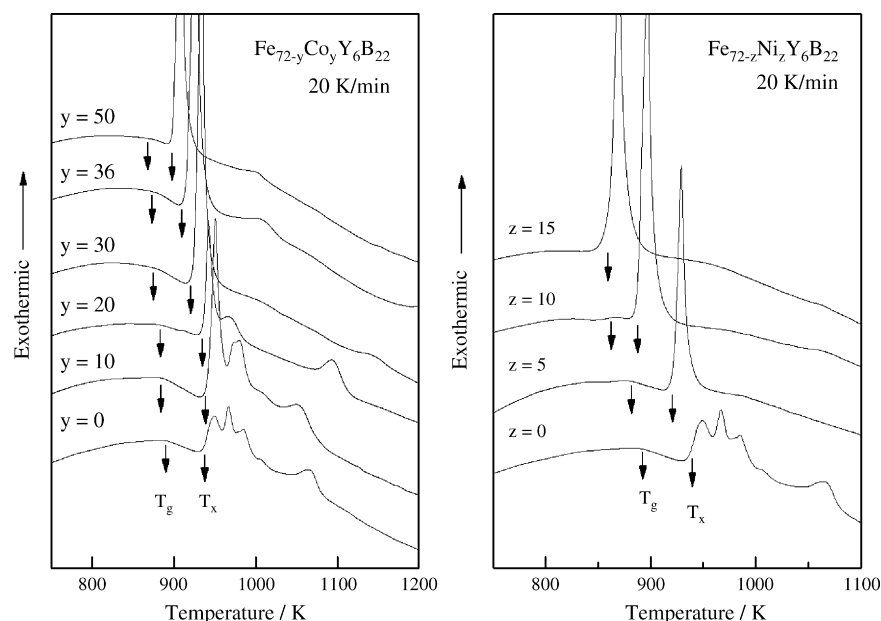


Fig. 3. DTA curves of  $\text{Fe}_{72-y}\text{Co}_y\text{Y}_6\text{B}_{22}$  ( $y=0, 10, 20, 30, 36, 50$ ) and  $\text{Fe}_{72-z}\text{Ni}_z\text{Y}_6\text{B}_{22}$  ( $z=0, 5, 10, 15$ ) amorphous ribbons.

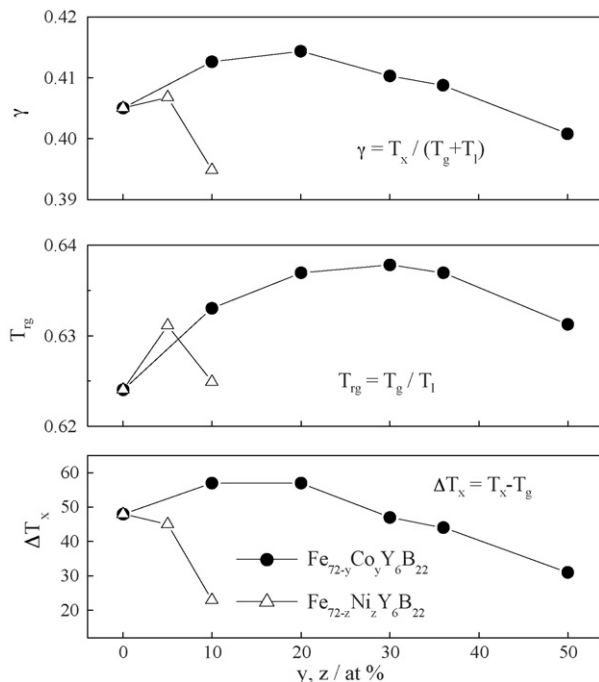


Fig. 4. Glass forming ability, expressed in different criteria, of Fe<sub>72-y</sub>Co<sub>y</sub>Y<sub>6</sub>B<sub>22</sub> ( $y = 0, 10, 20, 30, 36, 50$ ) and Fe<sub>72-z</sub>Ni<sub>z</sub>Y<sub>6</sub>B<sub>22</sub> ( $z = 0, 5, 10$ ) amorphous ribbons.

from 936 to 899 K while the glass transition temperature,  $T_g$ , slightly decreases from 888 to 868 K as Co addition is increased to 50 at.%. The liquidus temperature,  $T_l$ , gradually decreases from 1423 K to the lowest value of 1369 K as Co = 36 at.%. For Ni-modified system, with partial replacement of Fe by Ni, the  $T_x$  greatly decreases from 936 to 861 K as Ni is 15 at.%, and  $T_g$  decreases from 888 to 863 K as Ni is 10 at.% and finally vanishes as Ni is 15 at.%. The disappearance of  $T_g$  reveals the fact of decrement in GFA. The  $T_l$  was also lowered from 1423 to 1381 K with increasing Ni content. In these two systems, the  $T_x$  is high enough for operation at elevated temperature in industrial applications.

Fig. 4 shows the trend of several important factors for describing GFA of these two modified alloy systems. For the Co-modified system, the super-cooled liquid region,  $\Delta T_x$ , and  $\gamma$  factor increases to the maximum value 57 K and 0.414, respectively, as Co = 20 then decreases; while the reduced glass-transition temperature,  $T_{rg}$ , monotonically increases to the maximum value as Co = 30. In this system, both the  $\Delta T_x$ , and  $\gamma$  factors are consistent with the experimental results of GFA. For the Ni-modified system, the  $\Delta T_x$  monotonically decreases from 48 to 23 K with increasing Ni content, while  $T_{rg}$  and  $\gamma$  factors reach the maximum value as Ni = 10 at.%. Only  $\Delta T_x$  is consistent with the experimental results of GFA in the Ni substituted system. It is seen that the criteria for describing the GFA of an alloy developed to date are still not so satisfactory to precisely describe GFA of an alloy.

It has been found in literature that suitable Co addition improves the GFA of Fe-based BMG alloys [21,22]. This is also true in Fe–Co–Y–B alloy system. The addition of Co to replace Fe in Fe–Y–B alloys satisfies the above-mentioned three empirical rules [7]. The atomic size difference between Co and B atoms

is significant as the radius is 0.125 nm for Co and 0.09 nm for B atom. The addition of Co which is slightly smaller than Fe improves the degree of random packing structure of the alloy. The heat of mixing between Co and B pairs is  $-9$  kJ/mol [23]. The liquidus temperature is much lowered upon Co substitution leading to a higher  $T_g/T_l$  and  $\gamma$  factor. And the enlarged  $\Delta T_x$  also reveals a higher resistance against the crystallization. Experimental results indicate that these Co-containing alloys do exhibit better GFA. The complex crystallization behavior at 950–1000 K of the ternary Fe<sub>72</sub>Y<sub>6</sub>B<sub>22</sub> amorphous alloy, Fig. 3, turns to be simpler as increasing Co until converging into one as  $y = 30$ . While however the exothermic peaks at 1000–1150 K still exist. This depicts a possible crystallization of residual amorphous phase, or there exists a phase change between crystallized phases from ones with higher energy to new ones that have lower energy. These synergistic effects improve the GFA of the Co-containing alloys. On the contrary, being similar in atomic size with Co and the same heat of mixing with B (both  $-9$  kJ/mol), Ni addition causes manifest deterioration in GFA as reversed to that of Co addition. The fact is revealed by the decrement in attainable BMG diameter, the large decrement in  $\Delta T_x$  and the vanishing  $T_g$ . The crystallization mode becomes single, Fig. 3, being different from those of the ternary and Co-containing quaternary alloys. The three empirical rules of glass formation ability proposed earlier [7] fail to reasonably explain this discrepancy. It requires a further detailed investigation.

Fig. 5 shows hysteresis loops of the as-cast BMG rods measured by VSM. The saturation magnetization  $I_s$  linearly decreases from 1.47 T (Fe<sub>72</sub>Y<sub>6</sub>B<sub>22</sub>) to 1.11 T and to 0.95 T as the replacement of Fe is 36 at.% by Co and 20 at.% by Ni, respectively. From the measured loops of these two cases, one can see that the as-cast rods that are in amorphous state exhibit good soft magnetic properties such as extreme small  $H_c$  ( $<0.5$  Oe

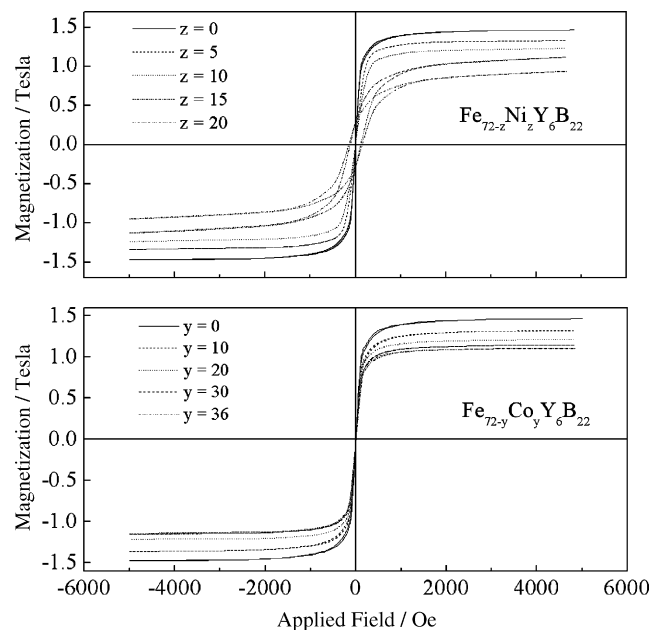


Fig. 5. M-H hysteresis loops taken from as-cast BMG rods, 1 mm in diameter, of Fe<sub>72-y</sub>Co<sub>y</sub>Y<sub>6</sub>B<sub>22</sub> ( $y = 0, 10, 20, 30, 36$ ) and Fe<sub>72-z</sub>Ni<sub>z</sub>Y<sub>6</sub>B<sub>22</sub> ( $z = 0, 5, 10, 15, 20$ ) alloys.



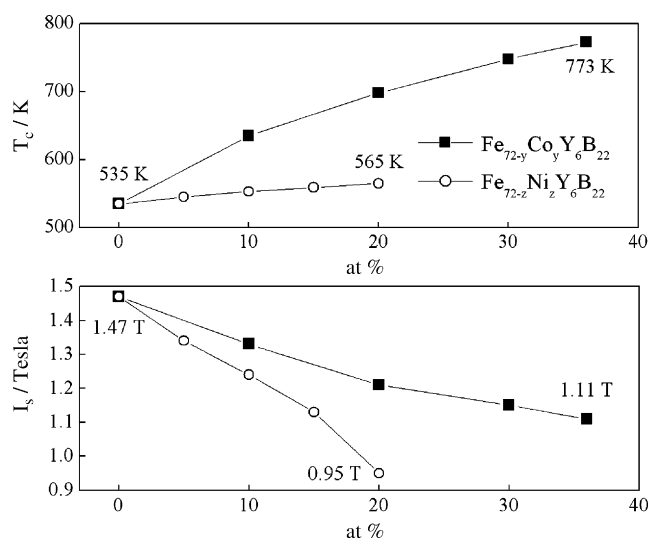


Fig. 6. Change in saturation magnetization,  $I_s$ , and Curie temperature,  $T_c$ , of  $\text{Fe}_{72-y}\text{Co}_y\text{Y}_6\text{B}_{22}$  ( $y=0, 10, 20, 30, 36$ ) and  $\text{Fe}_{72-z}\text{Ni}_z\text{Y}_6\text{B}_{22}$  ( $z=0, 5, 10, 15, 20$ ) BMG alloys.

or 40 A/m). However,  $H_c$  becomes significantly large, such as higher than 120 Oe as Ni = 15 and 20 at.% in which crystalline phases examined by XRD are dominating.

The trend of variation in saturation magnetization and Curie temperature,  $T_c$ , versus composition was summarized in Fig. 6. The Curie temperature,  $T_c$ , is also an important factor which is the higher the better to promise magnetic properties under the working temperature in industrial applications. The  $T_c$  greatly increases from 535 to 773 K as Co increases to 36 at.% while  $T_c$  slightly increases to 565 K as Ni is increased to 20 at.%. The Curie temperature,  $T_c$ , which depends on the interaction between magnetic atoms, increases manifestly with an increase in Co content as a result of the strong exchange coupling between Fe and Co atoms. The slight improvement of  $T_c$  with Ni replacement is proposed to be explained that the extremely large yttrium atoms (atomic radius  $r=0.227$  nm) pull apart the distance between Fe and Fe atoms ( $r=0.172$  nm) to a very large extent, so that the slightly smaller Ni atoms ( $r=0.162$  nm) partially compensate this distance to restore slightly the exchange interaction. The  $T_c$  of both investigated alloy systems is high enough for industrial applications.

The electrical resistivity ( $\rho$ ) that is the higher the better for industrial transformer applications was also measured on melt-spun ribbons. All studied amorphous alloys exhibit electrical resistivity higher than  $200 \mu\Omega \text{ cm}$ . The electrical resistivity increases to the maximum value of  $265 \mu\Omega \text{ cm}$  as Co content is 30 at.% then decreases;  $258 \mu\Omega \text{ cm}$  as Ni content is 20 at.%. The increment in electrical resistivity after adding Co or Ni into Fe–Y–B alloys may result from the increase of random atomic packing effect leading to an increased electron scattering effect. The results also show that electrical resistivity of the (Fe, Co, Ni)–Y–B amorphous alloys are almost five times that of silicon steels ( $\sim 50 \mu\Omega \text{ cm}$ ) and almost 2 times that of conventional Fe–Si–B amorphous ribbons ( $\sim 140 \mu\Omega \text{ cm}$ ). This reveals a great potential to highly reduce the eddy current loss under an alternative current, thus much lower iron loss is anticipated.

## 4. Conclusions

Thermal, glass forming ability and magnetic properties of ternary Fe–Y–B and Co or Ni modified Fe–Co–Y–B, Fe–Ni–Y–B quaternary bulk metallic glasses (BMGs) were studied. In  $\text{Fe}_{78-x}\text{Y}_x\text{B}_{22}$  BMG alloys, the  $T_g$  and  $T_x$  both increase with Y content from 843 to 928 K and 887 to 986 K, respectively; while the  $T_m$  and  $T_l$  remain almost unchanged with Y content. It showed that quaternary BMGs are possible when the replacement of Fe by Co is not higher than 36 at.%, or Ni replacement is not higher than 10 at.%. The good tolerance in GFA facilitates further modification in magnetic properties in (Fe, Co, Ni)–Y–B amorphous alloys to meet various applications. Both Co and Ni addition cause the decrement in  $T_x$  and  $T_g$ . The crystallization temperature,  $T_x$ , decreases from 936 to 899 K as Co = 36 at.%, while it greatly decreases from 936 to 861 K as Ni = 15 at.%. The glass transition temperature,  $T_g$ , decreases from 888 to 868 K as Co substitution is increased to 50 at.%; while it decreases from 888 to 863 K as Ni = 10 at.% and vanished as Ni = 15 at.%. Both Co and Ni lower the liquidus temperature of the Fe–Y–B alloys. The  $T_c$  increases linearly with Co or Ni content in both cases of replacement. The increase is manifest in case of Co, from 535 K (Co = 0%) to 773 K as Co = 36 at.%, and is slightly in case of Ni, 565 K as Ni = 20 at.%. Saturation magnetization decreases from 1.47 T (no Co, Ni) to 1.11 T as Co = 36 at.%, and to 0.95 T as Ni = 20 at.%. The coercive force of the studied BMGs is less than 0.5 Oe (40 A/m). Both systems exhibit electrical resistivity higher than  $200 \mu\Omega \text{ cm}$ . The electrical resistivity is  $265 \mu\Omega \text{ cm}$  and  $258 \mu\Omega \text{ cm}$  as Co = 30 at.% and Ni = 20 at.%, respectively. With the combination of the excellent properties, these (Fe, Co, Ni)–Y–B BMGs are very potential for industrial applications, such as cores for power transformers.

## Acknowledgment

The authors are grateful to the National Science Council, Taiwan, the Republic of China for sponsoring this research under the grant NSC 94-2216-E007-013.

## References

- [1] A. Inoue, K. Ohtera, K. Kita, T. Masumoto, Jpn. J. Appl. Phys. 27 (1988) L2248.
- [2] A. Inoue, T. Zhang, T. Masumoto, Mater. Trans. JIM 30 (1989) 965.
- [3] A. Inoue, T. Zhang, T. Masumoto, Mater. Trans. JIM 31 (1990) 177.
- [4] A. Peker, W.L. Johnson, Appl. Phys. Lett. 63 (1993) 2342.
- [5] A. Inoue, N. Nishiyama, T. Matsuda, Mater. Trans. JIM 37 (1996) 181.
- [6] T. Zhang, A. Inoue, Mater. Trans. JIM 39 (1998) 1001.
- [7] A. Inoue, Mater. Trans. JIM 36 (1995) 866.
- [8] K. Ikarashi, T. Mizushima, A. Makino, A. Inoue, Sci. Eng. A 304 (2001) 763.
- [9] H. Chiriac, N. Lupu, J. Magn. Magn. Mater. 215/216 (2000) 394.
- [10] T.D. Shen, R.B. Schwarz, Acta Mater. 49 (2001) 837.
- [11] C.Y. Lin, T.S. Chin, patent pending in Taiwan, Appl. (2004) No. 093109148 and in U.S. Appl. (2005) No. 11/138, 287.
- [12] C.Y. Lin, T.S. Chin, Appl. Phys. Lett. 86 (2005) 162501.
- [13] D. Xu, B. Lohwongwatana, G. Duan, W.L. Johnson, C. Garland, Acta Mater. 52 (2004) 2621.
- [14] D. Turnbull, Contemp. Phys. 10 (1969) 473.
- [15] D. Ma, H. Tan, D. Wang, Y. Li, E. Ma, Appl. Phys. Lett. 86 (2005) 191906.

- [16] H. Tan, Y. Zhang, D. Ma, Y.P. Feng, Y. Li, *Acta Mater.* 51 (2003) 4551.
- [17] D. Wang, Y. Li, B.B. Sun, M.L. Sui, K. Lu, E. Ma, *Appl. Phys. Lett.* 84 (2004) 4029.
- [18] D. Wang, H. Tan, Y. Li, *Acta Mater.* 53 (2005) 2969.
- [19] J. Zhang, H. Tan, Y.P. Feng, Y. Li, *Scripta Mater.* 53 (2005) 183.
- [20] M. Widom, M. Mihalkovic, *J. Mater. Res.* 20 (2005) 1.
- [21] A. Inoue, B.L. Shen, C.T. Chang, *Acta Mater.* 52 (2004) 4093.
- [22] J. Shen, Q. Chen, J. Sun, H. Fan, G. Wang, *Appl. Phys. Lett.* 86 (2005) 151907.
- [23] F.R. De Boer, R. Boom, W.C.M. Mattens, A.R. Miedema, A.K. Niessen, in: F.R. Boer De, D.G. Pettifor (Eds.), *Cohesion in Metals*, North-Holland, Amsterdam, 1989, p. 217.